0026-895X/05/6703-604–611$20.00
MOLECULAR PHARMACOLOGY
Copyright © 2005 The American Society for Pharmacology and Experimental Therapeutics
Mol Pharmacol 67:604–611, 2005

Vol. 67, No. 3
8672/1196871
Printed in U.S.A.

MOL PHARM

ACCELERATED COMMUNICATION

RSK4 and PAK5 Are Novel Candidate Genes in Diabetic Rat Kidney and Brain

Monika Niehof and Jürgen Borlak

Fraunhofer Institute of Toxicology and Experimental Medicine, Center for Drug Research and Medical Biotechnology, Hannover, Germany

Received October 27, 2004; accepted December 14, 2004

ABSTRACT

The orphan hepatic nuclear factor (HNF) HNF4α is of pivotal importance for liver development and hepatocellular differentiation and plays an essential role in a regulatory circuitry to control a wide range of metabolic processes. It also targets genes in other organs, including pancreas, kidney, intestine, and colon; promotes expression of an epithelial phenotype; triggers de novo formation of functional tight junctions; and contributes to epithelial cell polarity. In particular, HNF4α dysfunction leads to metabolic disorders, including diabetes. We used the chromatin immunoprecipitation (ChIP) cloning procedure and a bioinformatic approach to search for candidate genes associated with impaired liver, pancreas, and kidney function. We identified two novel targets regulated by HNF4α, which participate in the control, at least in part, in cell-cycle regulation and are members of the mitogen-activated kinase pathway. In multiple ChIP assays, ribosomal S6 kinase 4 (RSK4) and p21-activated kinase 5 (PAK5) were confirmed, and in vitro binding of HNF4α was evidenced by electrophoretic mobility shift assays (EMSA) using oligonucleotides, which harbor novel binding sites. We also used EMSA to probe for binding sites in promoters of HNF1α, apolipoprotein B, α1-antitrypsin, and angiotensinogen. We further studied RSK4 and PAK5 kinase expression in streptozotocin-induced diabetic rat kidney and brain and observed significant repression of HNF4α, RSK4, and PAK5 as determined by quantitative real-time reverse transcriptase-polymerase chain reaction. RSK4 and PAK5 may provide a molecular rationale for late-stage complications in disease, and further studies are warranted to explore these targets for the treatment of diabetic nephro- and neuropathy, frequently seen in patients with HNF4α dysfunction.

HNF4α is a zinc-finger transcription factor and regulates a large number of genes involved in lipid, steroid, xenobiotic, and amino acid metabolism (Sladek and Seidel, 2001; Schrem et al., 2002). This factor is of paramount importance for hepatocyte differentiation and organ development, and HNF4α knockout mice die at approximately embryonic day 9.5 because of impaired liver organogenesis (Chen et al., 1994; Li et al., 2000; Hayhurst et al., 2001; Parviz et al., 2003). The role of HNF4α in the glucose-dependent insulin secretory pathways is well recognized. Indeed, one form of a rare monogenetic disorder, termed maturity-onset diabetes of the young (MODY), was mapped to mutations within the HNF4α gene (MODY-1), thus confirming its role in pancreatic β-cell function (Sladek and Seidel, 2001; Schrem et al., 2002). Moreover, HNF4α dysfunction leads to multifactorial type 2 diabetes (Love-Gregory et al., 2004). Besides its pivotal functions in liver metabolism, HNF4α also targets genes in other tissues and organs including kidney, intestine, and colon (Sladek and Seidel, 2001). In general, HNF4α is a dominant regulator of an epithelial phenotype, triggers de novo formation of functional tight junctions, and contributes to epithelial cell polarity (Chiba et al., 2003). Because of its role in epithelial differentiation, it is probable that HNF4α functions in the control of cell proliferation as well. Little is known about disease-associated or disease-causing genes

This work was supported by a grant from the Lower Saxony Ministry of Culture and Science (to J.B.).
Article, publication date, and citation information can be found at http://molpharm.aspetjournals.org.
doi:10.1124/mol.104.008672.

ABBREVIATIONS: HNF, hepatic nuclear factor; RSK4, ribosomal S6 kinase 4; ChIP, chromatin immunoprecipitation; EMSA, electrophoretic mobility shift assay; MODY, maturity onset diabetes of the young; STZ, streptozotocin; NCBI, National Center for Biotechnology; RT-PCR, reverse transcriptase-polymerase chain reaction; PCR, polymerase chain reaction; bp, base pair(s); ApoB, apolipoprotein-B; AAT, α1-antitrypsin; ANG, angiotensinogen; PAK, p21-activated kinase; -pro suffix, promoter.

MOLECULAR PHARMACOLOGY
aspet
Downloaded from molpharm.aspetjournals.org by guest on December 1, 2012

MOL PHARM

MOLECULAR PHARMACOLOGY

targeted by HNF4α. In this study, we used the chromatin immunoprecipitation assay to search for novel HNF4α target genes in cultures of Caco-2 cells, and this colon carcinoma-derived cell line is well accepted for its usefulness in investigating HNF4α function and genes targeted by this factor (Soutoglou and Talianidis, 2002). In particular, we identified two disease-associated kinases (i.e., RSK4 and PAK5) that are regulated by HNF4α. This points to novel functions of this factor, which are beyond the regulation of genes involved in liver metabolism.

Materials and Methods

Caco-2 Cell Culture. Caco-2 cells were obtained from and cultivated as recommended by Deutsche Sammlung von Mikroorganismen und Zellkulturen GmbH (Braunschweig, Germany), seeded with a density of 4×10^6 cells/75 cm^2 flask, and harvested after 11 days.

Isolation of Nuclear Extracts, Western Blot Analysis, and Electrophoretic Mobility Shift Assays. The use of animals was approved by the local government of Hannover with project license 02-548. Sprague-Dawley rats ($n = 3$) were treated with a single intraperitoneal dose of 100 mg of Aroclor 1254 per kilogram of body weight and killed 72 h later. Nuclear extracts from rat liver were prepared as described by Gorski et al. (1986), whereas nuclear extracts from Caco-2 cells were isolated by the method used by Dignam et al. (1983) with minor modifications as detailed previously (Niehof et al., 2001). For Western blot analysis, nuclear extracts were separated on a 12% SDS-polyacrylamide gel and blotted onto a polyvinylidene difluoride membrane. Antibody directed against HNF4α was purchased from Santa Cruz Biotechnology (Heidelberg, Germany). The antigen-antibody complexes were visualized using the ECL detection system as recommended by the manufacturer (PerkinElmer Life and Analytical Sciences, Rodgau-Juegesheim, Germany), and chemiluminescence was recorded with Kodak IS 440 CF (Biostep GmbH, Jahnsdorf, Germany). Electrophoretic mobility shift assays were performed as described previously (Niehof et al., 2001). Binding buffer consisted of 25 mM HEPES, pH 7.6, 5 mM $MgCl_2$, 34 mM KCl, 2 mM dithiothreitol, 2 mM Pefabloc, 2% aprotinin, 40 ng/μl poly(dI-dC), and 100 ng/μl bovine serum albumin. The oligonucleotides were purchased from MWG Biotech (Ebersberg/Munich, Germany) and used as ^{32}P-labeled probes; for sequence information, see Table 1. Supershift experiments were done with an HNF4α-specific antibody (Santa Cruz Biotechnology).

Cross-Linking and Chromatin Immunoprecipitation. All chromatin immunoprecipitation (ChIP) procedures were carried out as described by Weinmann et al. (2001) with some modifications. The samples were sonicated on ice until cross-linked chromatin was fragmented to approximately 0.2 to 1.6 kilobase pairs. Protein A-Sepharose CLB4 (Amersham Biosciences, Freiburg, Germany) was blocked with 1 mg/ml bovine serum albumin and 1 mg/ml herring sperm DNA (Promega, Mannheim, Germany) and washed extensively before use. Chromatin preparations were precleared by incubation with "blocked" Protein A-Sepharose for 1 h at 4°C. Precleared chromatin from 2.5×10^7 cells was incubated with 1 μg of HNF4α antibody or no antibody and rotated at 4°C overnight. After recovering of immunocomplexes, extensive washing, and elution, two samples were pooled for a second immunoprecipitation step with the HNF4α antibody. PCR was done in a mixture containing 2 μl of purified DNA or 2 μl of a 1:200 dilution of the total input sample, 1 μM of each primer, 0.25 mM dNTP mixture, 0.625 U Thermostart-Taq (ABgene, Hamburg, Germany), and 1× PCR buffer (ABgene; with 1.5 mM $MgCl_2$) in a total volume of 20 μl. PCRs were carried out with a T3 Thermocycler (Biometra, Göttingen, Germany) with the following conditions: initial denaturation at 95°C for 15 min (Thermostart activation), denaturation at 94°C for 30 s, annealing at different temperatures for 45 s (Table 2), extension at 72°C for 45 s, final extension at 74°C for 10 min, 45 cycles. A detailed account of PCR primers to analyze immunoprecipitated target genes is given in Table 2. We used two rounds of sequential chromatin immunoprecipitations (Weinmann et al., 2001) to increase purity and specificity of target DNA for ChIP-cloning and for validation of ChIP-derived clones. Other investigators used a single immunoprecipitation step with obvious limitations for validation of targets (Horak et al., 2002; Tomaru et al., 2003). In numerous independent ChIP experiments, immunoprecipitated DNA contained the full complement of selected HNF4α target genes (HNF1α, ApoB, AAT, and ANG), which served as our positive controls. For a novel candidate gene, we demanded at least three independent confirmations from a series of independent ChIP experiments until a candidate gene was considered to be confirmed.

Cloning and Sequence Analysis. The immunoprecipitated DNA was treated with T4 DNA polymerase (New England Biolabs, Frankfurt, Germany) to create blunt ends, purified, and cloned into the zero-blunt vector (Invitrogen, Karlsruhe, Germany) using the zero-blunt PCR cloning kit (Invitrogen) according to the manufacturer's recommendations. Colonies having inserts were identified by restriction-enzyme digestion using enzymes in the polylinker. Plasmid DNA was purified with QIAquick PCR Purification Kit (QIAGEN GmbH, Hilden, Germany), subjected to cycle sequencing with vector-specific primers using BigDyeTerminator v3.1 Kit, and injected into ABI 3100 Genetic Analyzer (Applied Biosystems, Darmstadt, Germany). Sequences were identified and annotated by database searches (GenBank version build 34, maintained by NCBI). Detailed sequence information is given in Table 3.

Bioinformatic Searching for HNF4α Binding Sites. The transcription start site (+1) of the NCBI mRNA reference sequence was used for promoter annotation of the respective clones. Cloned fragments and respective proximal promoters (−1 to −3000 bp) were checked for putative HNF4α binding sites with two different bioinformatic weight matrix-based tools: V$HNF4_01 with cut-off core similarity 0.75 and matrix similarity 0.78, Transfac matrix (Biobase, Wolfenbüttel, Germany), and V$HNF4_01 with cut-off core similarity 0.75 and matrix similarity 0.82 or V$HNF4_02 with cut-off core similarity 0.75 and matrix similarity 0.76, Genomatix matrix (Genomatix Software GmbH, München, Germany).

TABLE 1
Shift-probe sequences

Gene/Clone	Oligonucleotide Name	Sequence
HNF1α	HNF1pro	AAGGCTGAAGTC**CAAAG**TTCAGTCCCTTC
α1-Antitrypsin	AATpro	CAACAGGGG**CTAAG**TCCACTGGC
Apolipoprotein B	ApoBpro	GGAAAGGTC**CAAAG**GGCGCCTTG
Angiotensinogen	ANGpro	TGCAGAGGG**CAGAG**GGCAGGGGA
Clone 113, site a	GS09	TGTTGGGTA**CAATG**TTCAATATT
Clone 113, site b	GS16	AAAGCTGAC**TAAGG**TACATGTGC
Clone 113/prosite a	GS04	GAGCTGGGA**CAAAA**ACTCAGACT
Clone 113/prosite b	GS46	TTAAGTGAT**TAAAG**TTCAATATT
Clone 113/prosite c	GS29	TGTGGTGGA**CAAAG**GAATGTTTT
Clone 23/prosite a	GS26	AATGGAGGG**CATAG**GTCAACAGC
Clone 23/prosite b	GS27	CCAGCGCT**CAAAA**GGTTGGCAGT

Downloaded from molpharm.aspetjournals.org by guest on December 1, 2012

aspet

RT-PCR and Real-Time RT-PCR. Total RNA was isolated using the nucleospin RNA Isolation Kit (Macherey-Nagel, Düren, Germany) according to the manufacturer's recommendations. Total RNA from each sample (4 μg) was used for reverse transcription (Omniscript Reverse Transcriptase, QIAGEN GmbH). PCR was done in a mixture containing a cDNA equivalent to 25 ng of total RNA, 1 μM concentrations of each primer, 0.25 mM dNTP mixture, 0.625 U Thermostart-Taq (ABgene), and 1× PCR buffer (ABgene; with 1.5 mM $MgCl_2$) in a total volume of 20 μl of PCR. PCRs were carried out with a thermocycler (T3; Biometra) with the following conditions: initial denaturation at 95°C for 15 min (Thermostart activation), denaturation at 94°C for 30 s, annealing at different temperatures for 45 s (Table 4), extension at 72°C for 45 s, and final extension at 74°C for 10 min. Various cycle numbers were used to demonstrate linearity, and 40 cycles were used for tissue comparison. A detailed oligonucleotide sequence information is given in Table 4.

Real-Time Semiquantitative PCR. Real-time RT-PCR measurement was done with the Lightcycler (Roche Diagnostics, Mannheim, Germany) with the following conditions (Table 5): denaturation at 94°C for 120 s, annealing at different temperatures for 8 s, extension at 72°C for different times, and fluorescence at different temperatures. The PCR reaction was stopped after a total of 30 to 50 cycles, and at the end of each extension phase, fluorescence was observed and used for quantitative measurements within the linear range of amplification. Exact quantification was achieved by serial dilution with cDNA produced from total RNA extracts using 1:5 dilution steps. A detailed oligonucleotide sequence information is given in Table 5. Gene expression levels were normalized to *mitATPase6*, which we found to be stably expressed.

Diabetic Disease Model. Streptozotocin (STZ) is a well-known β-cell toxin that results in diabetes. Kidneys of STZ-treated Sprague-Dawley rats (6 months of treatment) were kindly provided by R. Amann (Institute of Pathology, University of Erlangen, Erlangen, Germany). Conclusive evidence for this treatment to result in diabetic nephropathy was published recently (Gross et al., 2003). Experimental diabetes was induced by single intravenous injection of 65 mg of STZ/kg body weight. All injected animals developed hyperglycemia on day 2 after STZ administration. Thereafter, diabetic animals were treated daily with 4.1 ± 1.4 IU/kg of body weight of long-acting insulin (Gross et al., 2003). Diabetic rats had stable, moderate hyperglycemia throughout the 6 months (mean blood glucose concentrations, 650 ± 104 mg/dl) (Gross et al., 2003). Furthermore, liver, kidney, and brain of STZ-treated Wistar rats (2 months of treatment) were kindly provided by P. Rösen (German Diabetes Research Institute, Düsseldorf, Germany). Experimental diabetes was induced by single intraperitoneal injection of 60 mg of STZ/kg of body weight. All animals developed hyperglycemia until 60 h after STZ injection. The animals did not receive an antidiabetic treatment. Diabetic rats had stable, moderate hyperglycemia throughout the 2 months (mean blood glucose concentrations, >400 mg/dl) (Dhein et al., 2003). After 2 months, the experiment was terminated.

Results and Discussion

We used the ChIP cloning procedure to identify novel HNF4α target genes after formaldehyde cross-linking of nucleoprotein complexes in highly differentiated Caco-2 cell cultures (Hu and Perlmutter, 1999) (Fig. 1A). At day 11 in culture, the HNF4α protein expression was abundant (Fig. 1B), as determined by Western blotting experiments. Furthermore, EMSA experiments evidenced a marked increase in HNF4α DNA binding to the A site of the *HNF1α* promoter (HNF1pro) (Fig. 1C). The A site is an established recognition site for HNF4α (Sladek and Seidel, 2001; Schrem et al., 2002). The ability of the HNF4α antibody to immunoprecipitate HNF4α was confirmed by Western blotting (Fig. 1D), and specificity of the ChIP assay was tested for by screening of immunoprecipitated DNA for enrichment of promoter se-

TABLE 2
ChIP-PCR primer sequences and amplification settings

Gene/Clone	Primer Name	Primer Direction	Primer Sequence	Fragment Length	Annealing Temp.
				bp	*°C*
HNF1α	Ni16	Forward	CATGATGCCCCTACAAGGTT	274	60
		Reverse	ATTGGAGCTGGGGAAATTCT		
ApoB	Ni56	Forward	GAGGCTCTTCAAGGCTCAAA	181	60
		Reverse	AACCGAGAAGGGCACTCAG		
AAT	Ni75	Forward	GGAACAGCCACTAAGGATTCTGCAGTGAG	380	60
		Reverse	TCACTGTCCCAGGTCAGTGGTGGTGCCTG		
ANG	Ni117	Forward	GGGAGATGTACCCCCAAGAG	200	60
		Reverse	GCTTGTGTGTTTTCCCCAGT		
Clone 23, prosite a	Ni8	Forward	CCAACTCAGGACCTTGGAGA	141	60
		Reverse	GGCCAGCTTTGCTTCATTAG		
Clone 23, prosite b	Ni13	Forward	GAGCTGCTGTGCCTGGTACT	148	60
		Reverse	TTTTTGCTGACGGGAGAGAT		
Clone 113, site a	Ni61	Forward	TCATCACGGACATAAAGATGGA	160	60
		Reverse	GCATAGTGGTGGGGGTTCT		
Clone 113, site b	Ni73	Forward	AGCAGAACCCCCACCACTAT	187	60
		Reverse	TCACCCAGAAAGTTCCCTTG		
Clone 113, prosite a	Ni5	Forward	CCGGTCAAGTCTGAACCAGT	126	60
		Reverse	TTAACTAGGCAAGCCCAAGC		
Clone 113, prosite c	Ni116	Forward	TAGTCCCTGTGGCTGCAGTA	232	60
		Reverse	TCTCAATGGCTGATTACAGGTT		

TABLE 3
Sequence information of clones

Clone	Gene Name	Accession Number	Chromosome	Base pairs Relative to Transcription Start Site[a]
23	RSK4/RPS6KA6	NM_014496	X	+13,768 to +14,368
113	PAK5/PAK7	NM_045653	20	+246,494 to +246,839

[a] NCBI GenBank Version Build 34.

MOL PHARM
MOLECULAR PHARMACOLOGY
aspet
Downloaded from molpharm.aspetjournals.org by guest on December 1, 2012

MOL PHARM

MOLECULAR PHARMACOLOGY

quences of well-known HNF4α target genes (Sladek and Seidel, 2001; Schrem et al., 2002). In particular, we confirmed by PCR amplification that immunoprecipitated DNA contains *HNF1α*, apolipoprotein-B (*ApoB*), α1-antitrypsin (*AAT*), and angiotensinogen (*ANG*) (Fig. 1E). We therefore provide evidence for the enrichment of known HNF4α target genes in immunoprecipitated DNA and document specificity for the experimental procedure. We further evidence expression of HNF4α target genes by RT-PCR (Fig. 1F), and for each ChIP assay, detection of the HNF1 prosite served as a positive control. We thoroughly validated our experimental approach before the cloning of immunoprecipitated DNA and ChIP assays yielded clones with inserts of up to 1800 bp. The inserts were sequenced with vector-specific primers, and the genomic sequences were identified by database searches (GenBank, maintained by NCBI). We found novel HNF4α target genes distributed among different chromosomes. This demonstrates the usefulness of ChIP cloning procedure to identify multiple chromosomal targets for this factor. Some of the cloned fragments were within intronic regions, and this agrees well with findings by other investigators (Greenbaum and Zhuang, 2002; Martone et al., 2003; Solano et al., 2003). We also analyzed proximal promoter sequences. Cloned fragments as well as promoter sequences were checked for putative HNF4α binding sites, and primer pairs were designed to confirm experimentally predicted sites. Independent ChIP experiments followed by PCR analyses with clone-specific or promoter-specific primers enabled robust identification of HNF4α target genes.

Here, we report in detail the identification of two novel kinases targeted by HNF4α. Binding in vivo of HNF4α was confirmed for two recognition sites of clone 113 (Fig. 2A). In addition, by using a bioinformatic approach, we predicted promoter binding sites within clones 113 and 23, which were specifically bound by HNF4α in vivo (Fig. 2A). We further studied the ability of HNF4α to bind to cognate recognition sites by EMSA with ^{32}P-labeled probes encompassing the predicted HNF4α sites located in clone 113 (GS09, GS16), in the promoter of clone 113 (GS04, GS29), and in the promoter of clone 23 (GS26, GS27) (Fig. 2B). Supershift experiments with a specific HNF4α antibody resulted in strong binding of HNF4α with probes GS09, GS16, and GS26 and weaker binding with probe GS27. No binding of HNF4α was detected with probes GS04 and GS29. Competition and supershift experiments with probes specific for several HNF4α target genes were carried out to estimate binding affinity of HNF4α to known and newly identified targets (Fig. 2, B and C). Again, the HNF1 prosite was used as labeled probe, and competition was first analyzed with different known cognate recognition sites, namely the HNF1 prosite itself and HNF4α binding sites within AATpro, ApoBpro, and ANGpro. These sites were distinguishable in their binding affinity (Fig. 2C). With the AAT prosite (100×, reduction to 10%) and the ApoB site (100×, reduction to 2.5%), binding was comparable with

TABLE 4
RT-PCR primer sequences and amplification settings

Gene/Clone	Primer Name	Accession Number	Primer Direction	Primer Sequence	Fragment Length	Annealing Temp.
					bp	*°C*
HNF1α human	Th#55	NM_000545	Forward	TCTACAACTGGTTTGCCAACC	313	50
			Reverse	GGCTTCTGTACTCAGCAGGC		
ApoB human	Ni94	NM_000384	Forward	TTCAGTGTGGACAGCCTCAG	350	60
			Reverse	CATGGTTTGGCCCATATTTC		
AAT human	Ni24	NM_000295	Forward	AGGGCCTGAAGCTAGTGGAT	423	58
			Reverse	GGTGCTGTAGTTTCCCCTCA		
ANG human	Th#83	NM_000029	Forward	GGATGAGAGAGAGCCCACAG	351	60
			Reverse	CTCACTCCATGCAGCACACT		
Clone 23 human	Ni69	NM_014496	Forward	GGATTTTCTCAGGGGAGGAG	311	60
			Reverse	AATCAGCACTCTGGGAATGG		
Clone 113 human	Ni72	NM_020341	Forward	GAATCAGACAAGCCCTCAGC	309	55
			Reverse	CCAGACGGGTACTGGTGACT		
HNF4α human	Th#588	NM_178849	Forward	CTGCTCGGAGCCACAAAGAGATCCATG	370	50
			Reverse	ATCATCTGCCACGTGATGCTCTGCA		
Clone 23 rat	Ni126	XM_228473	Forward	AATTGGCCCTAGCTTTGGAT	217	60
			Reverse	CTCTGAGAATGGCCTCTTCG		
Clone 113 rat	Ni127	XM_230625	Forward	AGACCCCAGGGAATATTTGG	240	56
			Reverse	ATGACCACCCAGAGCTCATC		
HNF4α rat	Th#84	NM_022180	Forward	GCCTGCCTCAAAGCCATCAT	274	55
			Reverse	GACCCTCCAAGCAGCATCTC		

TABLE 5
Real-time PCR primer sequences and amplification settings

Gene/Clone	Accession Number	Primer Direction	Primer	Fragment Length	Annealing Temp.	Extension	Fluorescence
				bp	*°C*	*s*	
Clone 23 rat (Ni126)	XM_228473	Forward	AATTGGCCCTAGCTTTGGAT	217	68	9	82
		Reverse	CTCTGAGAATGGCCTCTTCG				
Clone 113 rat (Ni127)	XM_230625	Forward	AGACCCCAGGGAATATTTGG	240	68	10	84
		Reverse	ATGACCACCCAGAGCTCATC				
HNF4α rat (Th#84)	NM_022180	Forward	GCCTGCCTCAAAGCCATCAT	274	55	11	88
		Reverse	GACCCTCCAAGCAGCATCTC				
MitATPase6 (Th#643)	AF115770	Forward	CTAAAGGACGAACCTGA	315	55	13	83
		Reverse	TGGCCTGCAGTAATGTT				

aspet

Downloaded from molpharm.aspetjournals.org by guest on December 1, 2012

the HNF1 prosite itself (100×, reduction to 2.2%), whereas competition with the ANG prosite (100×, reduction to 34.6%) was less efficient. In comparison, competition with the GS09 probe (100×, reduction to 13.7%) and the GS26 probe (100×, reduction to 9.5%) resulted in strong binding, whereas competition with the GS16 probe (100×, reduction to 32.5%) was less efficient, and binding affinity with the GS27 probe (100×, reduction to 85.8%) was minimal. In addition, we performed experiments with GS08 as the ^{32}P-labeled probe, and competition was performed with probes for the known cognate recognition sites, namely HNF1pro, ApoBpro, AATpro, and ANGpro (Fig. 2C). All probes competed successfully for HNF4α binding (100×, with HNF1pro reduction to 4.7%, with ApoBpro reduction to 4.5%, with AATpro reduction to 6.6%, and with ANGpro reduction to 8.6%). Competition experiments were complemented by supershift assays. Clone 113 itself and two sites in the promoter of clone 23 were thus confirmed for in vivo and in vitro binding of HNF4α.

It is noteworthy that we did not confirm HNF4α in vitro binding for certain putative sites (prosites a and c) in the promoter of clone 113. Nonetheless, the surrounding regions of 126 and 232 bp contained in vivo binding sites (Fig. 2A). The promoter thus harbors an adjacent HNF4α binding site (prosite b, GS46, localized approximately 800 bp upstream to site a and approximately 400 bp downstream to site c), exhibiting strong in vitro binding of HNF4α (Fig. 2, B and C), which would allow for immunoprecipitation of prosite a and prosite c through protein-protein cross-links. Indeed, HNF4α may contact DNA through various protein-protein interactions, particularly through cooperative binding with synergized factors, because formaldehyde cross-links leads to both protein-DNA and protein-protein complexes. Therefore in ChIP experiments, a three-dimensional, higher-order structure can be cross-linked. In addition, HNF4α may also contact another site within the in vivo confirmed fragments, which was not predicted by our computational approach.

It is noteworthy that gene regulation of a broad range of cytochrome P450 isozymes does depend on promoter activation by HNF4α (Jover et al., 2001), and treatment of hepatocytes with Aroclor 1254 resulted in the induction of HNF4α and several cytochrome P450 mono-oxgenases (Borlak and Thum, 2001). We therefore analyzed HNF4α binding in liver nuclear extracts of control and Aroclor 1254-treated rats by EMSA. Binding of HNF4α to HNF1pro as well as to the newly identified binding sites (GS09, GS16, GS46, GS26, and GS27) was significantly increased after Aroclor 1254 treatment (Fig. 2D), thus providing additional evidence for our novel targets to be strictly regulated by HNF4α.

A summary of the cloned HNF4α targets is given in Table 6. Clone 23 contained two ChIP-verified HNF4α binding sites in the promoter region (around −1430 and −2053) and was identified as *RSK4*, a novel member of the ribosomal S6 kinase subfamily (Yntema et al., 1999; Kohn et al., 2003). Because RSK4 gene deletion was found in some patients with X-linked mental retardation, a role for this kinase in neuronal development was suggested (Yntema et al., 1999). RSK4 expression during mouse development, however, is ubiquitous (Kohn et al., 2003), which suggests additional roles for the gene product in development. Clone 113 contained two ChIP-verified HNF4α promoter binding sites around −951

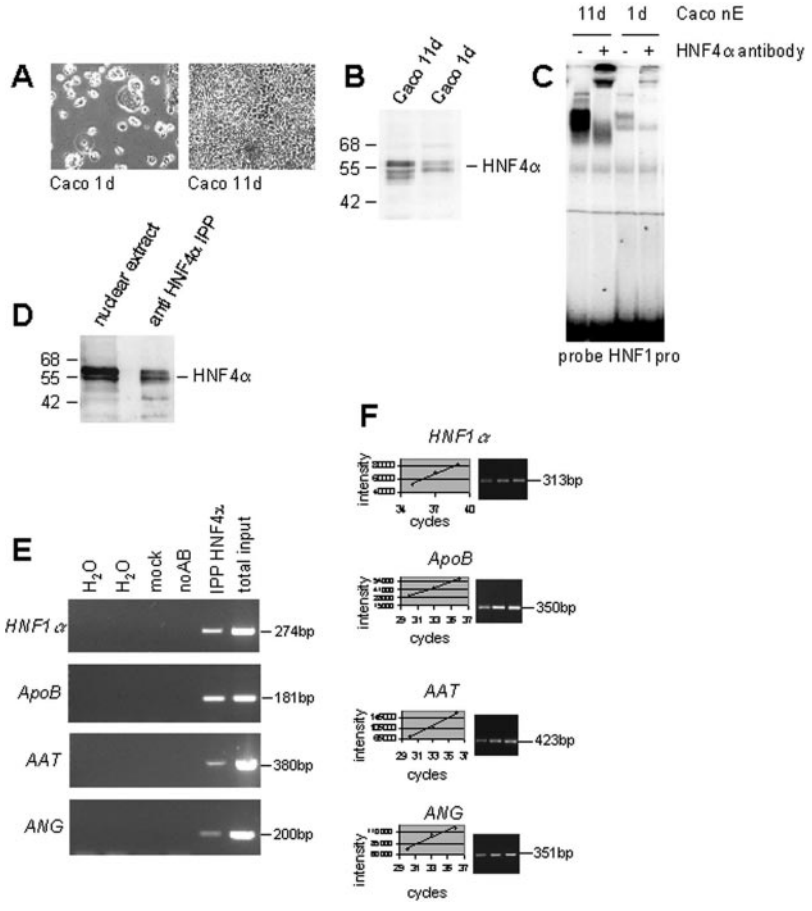

Fig. 1. HNF4α chromatin immunoprecipitation assay with HNF4α target genes. A, phase-contrast photomicrographs of cultured Caco-2 cells at days 1 and 11 (magnification, 200×). B, HNF4α Western blotting analysis of 30 μg of Caco-2 cell nuclear extracts prepared at day 1 or 11. C, electrophoretic mobility shift experiment with 2.5 μg of Caco-2 cell nuclear extracts prepared at day 1 or 11 and an oligonucleotide corresponding to the A site of the *HNF1α* promoter (HNF1pro) as ^{32}P-labeled probe. For supershift analysis, an antibody directed against HNF4α was added. D, HNF4α Western blot analysis of 30 μg of total nuclear extract and of HNF4α immunoprecipitated complexes (anti-HNF4α IPP) of Caco-2 cells. E, ChIP experiments were performed with cultured Caco-2 cells and an antibody against HNF4α (IPP HNF4α) or no antibody (no AB). The no-antibody control was used to monitor unspecific binding of DNA. After DNA purification, samples were subjected to PCR with primers designed to amplify promoters of different HNF4α-positive targets. The primers annealed proximal to the HNF4α binding sites of the *HNF1α* promoter, the apolipoprotein B (*ApoB*) promoter, the α1-antitrypsin (*AAT*) promoter, and the angiotensinogen (*ANG*) promoter, all of which are well-known HNF4α targets. A mock probe and a portion of the total input sample were also examined by PCR. A mock probe, containing buffer without chromatin, was treated categorically throughout the whole immunoprecipitation procedure and throughout DNA isolation and purification to control for external DNA contamination. Two reactions containing H_2O instead of template were routinely included in each PCR as negative control. F, gene expression of *HNF1α*, *ApoB*, *AAT*, and *ANG* in cultures of Caco-2 cells was analyzed by RT-PCR. A linear range of amplification cycles is shown.

MOL PHARM
MOLECULAR PHARMACOLOGY
aspet
Downloaded from molpharm.aspetjournals.org by guest on December 1, 2012

and −2181 and was conclusively annotated as *PAK5*. This kinase was recently cloned and characterized as a novel member of mammalian p21$^{cdc42/rac1}$-activated kinase subfamily (Dan et al., 2002; Pandey et al., 2002). Until now, its role was confined to the induction of neurite outgrowth (Dan et al., 2002), whereas PAK kinases, in general, play a role in neurodegenerative diseases (Kumar and Vadlamudi, 2002).

It is of considerable importance that HNF4α targets kinases important in neuronal development and function. Thus, besides its role in liver metabolism, HNF4α may also play a role in brain function. In particular, HNF4α regulates several genes involved in glucose metabolism (Sladek and Seidel, 2001; Schrem et al., 2002) and participates in the glucose-dependent insulin secretory pathways. HNF4α dysfunction, however, does lead to multifactorial type 2 diabetes (Love-Gregory et al., 2004) with patients developing diabetic neuropathies. Moreover, one form of a rare monogenetic disorder, MODY, was mapped to mutations within the HNF4α gene (MODY-1) (Sladek and Seidel, 2001; Schrem et al., 2002). Patients with diabetes harbor a high risk for progressive neuropathies for uncertain reasons (Vinik et al., 2000). Although the precise role of HNF4α in brain function is unknown, we demonstrate gene expression of this transcription factor in human and rat brain (Fig. 2E). It is interesting that expression of the splice variant HNF4α7 was also reported for mouse brain (Nakhei et al., 1998). Next to its expression in brain tissue, *RSK4* is expressed at a similar level in kidney but lesser in pancreas and placenta (Yntema et al., 1999). We provide strong evidence for RSK4 to be expressed in Caco-2 cells, in human and rat liver, and in rat kidney (Fig. 2E). Unlike *RSK4*, *PAK5* is abundantly expressed in pancreas, but the level of expression is minimal in liver and kidney (Dan et al., 2002). We demonstrate expression of *PAK5* in RNA extracts of human and rat liver and in

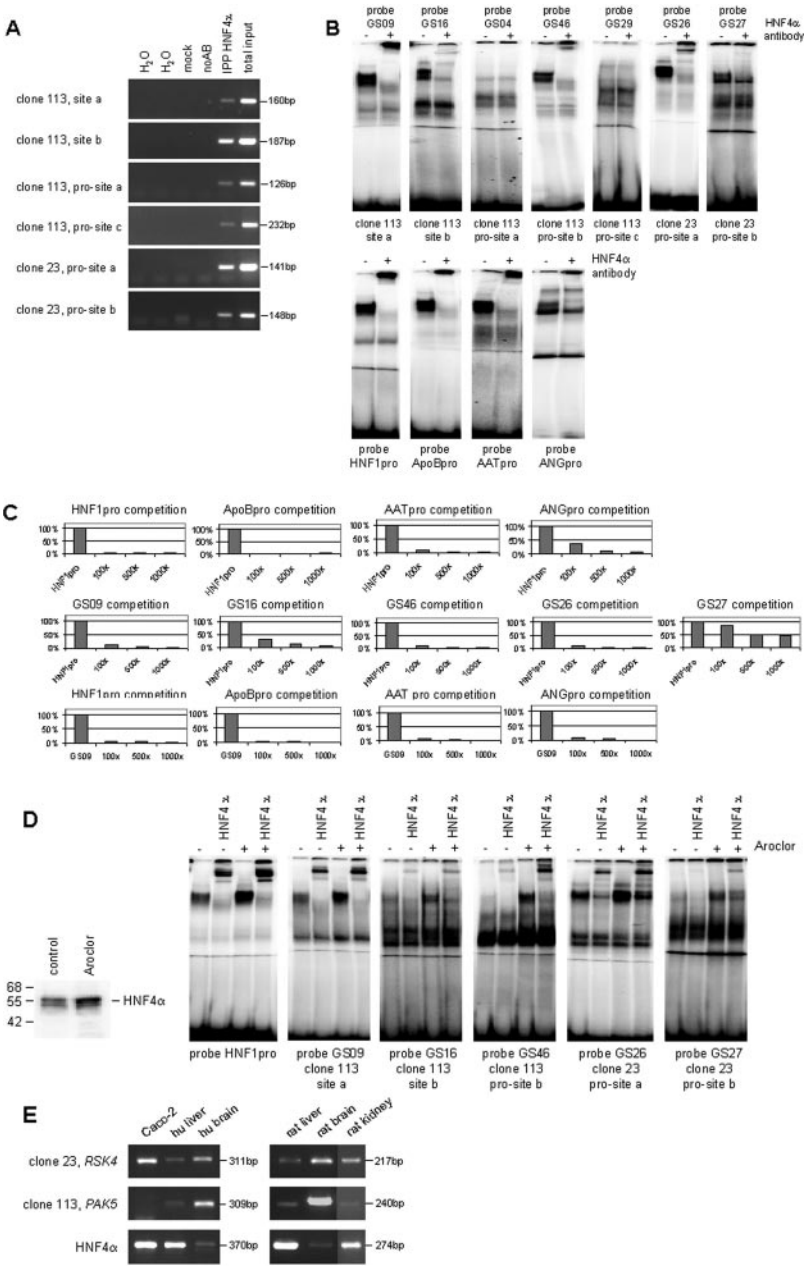

Fig. 2. Confirmation of ChIP clones by examination of HNF4α binding in vivo and in vitro. A, independent ChIP experiments were performed with cultures of Caco-2 cells and an antibody against HNF4α (IPP HNF4α) or no antibody (no AB). After DNA purification, samples were subjected to PCR with primers designed for putative HNF4α binding sites of clones and their promoters (clone 113, clone 113 prosite a and prosite c, clone 23 prosite a and prosite b). A mock probe and an aliquot of the total input sample were also examined by PCR. B, electrophoretic mobility shift assays with 2.5 μg of Caco-2 cell nuclear extract and oligonucleotides (GS09, GS16, GS04, GS46, GS29, GS26, and GS27) corresponding to putative HNF4α binding sites within the identified clones and promoters and with the A site of the *HNF1*α promoter (HNF1pro), the HNF4α binding-site of the α1-antitrypsin promoter (AATpro), the HNF4α binding-site of the apolipoprotein B promoter (ApoBpro), and the C-region of the angiotensinogen promoter (ANGpro) as ^{32}P-labeled probe. In supershift assays, an antibody directed against HNF4α (+) was added. C, competition experiments. Electrophoretic mobility shift experiments were carried out with 2.5 μg of Caco-2 cell nuclear extracts and an oligonucleotide corresponding to the A site of the *HNF1*α promoter or to the putative HNF4α binding site GS09 as ^{32}P-labeled probe. The A site of the HNF1pro, the HNF4α binding site of AATpro, the HNF4α binding site of ApoBpro, the C region of ANGpro, or the putative HNF4α binding sites (GS09, GS16, GS46, GS26, and GS27) were added as 100-, 500-, and 1000-fold molar excess. Dried gels were analyzed with a Molecular Imager using the Quantity One software (Bio-Rad, Hercules, CA). HNF4α binding to the A site of the *HNF1*α promoter or to the putative HNF4α binding site GS09 as ^{32}P-labeled probe was set to 100%, and competition was quantified for each oligonucleotide. D, HNF4α Western blot analysis (left) of 30 μg of liver nuclear extract of control and Aroclor-treated rats. Electrophoretic mobility shift assay with 2.5 μg of rat liver nuclear extract of control or Aroclor-treated animals and oligonucleotides corresponding to different potential HNF4α binding sites (HNF1pro, GS09, GS16, GS46, GS26, and GS27) as ^{32}P-labeled probe. In supershift assays, an antibody directed against HNF4α was added. E, gene expression of clone 23 (*RSK4*), clone 113 (*PAK5*), and *HNF4*α was analyzed by RT-PCR in extracts of Caco-2 cell cultures, human liver, human brain, rat liver, rat brain, and rat kidney. In the case of PAK5, half of the PCR reaction was loaded on the gel for human and rat brain; in the case of HNF4α, half of the PCR reaction was loaded on the gel for Caco-2 cells, human liver, rat liver, and kidney.

Downloaded from molpharm.aspetjournals.org by guest on December 1, 2012

MOL PHARM

MOLECULAR PHARMACOLOGY

rat kidney (Fig. 2E) but not in cultures of Caco-2 cells. Failure to detect *PAK5* mRNA transcripts in Caco-2 cells suggests lack of synergistic transcription factors acting in concert, even though in vivo binding of HNF4α to *PAK5* recognition sites was confirmed (Fig. 2A).

HNF4α is a dominant regulator of the epithelial phenotype and is highly expressed in kidney (Sladek and Seidel, 2001). Furthermore, in diabetic patients, nephropathy is a frequently observed complication, and treatment of rats with STZ results in diabetic nephro- and neuropathy (Gross et al., 2003; Bianchi et al., 2004). We observed significant reduction of *HNF4α* transcript level in liver. Likewise, *PAK5* gene expression in brain extracts of STZ-induced diabetic rats was repressed, as was *HNF4α* itself, *RSK4*, and *PAK5* in total RNA extracts of rat kidney (Table 7). We therefore demonstrate diabetic neuropathy and nephropathy to be strongly associated with repressed *RSK4* and *PAK5* gene expression levels, as a result of HNF4α dysfunction. It is noteworthy that treatment of rats with Aroclor 1254 led to significant induction of *RSK4* mRNA in rat kidneys (Table 7), thus providing further evidence for a coordinate regulation of RSK4 and HNF4α gene expression.

In general, members of the RSK family function as downstream mediators of mitogen-activated protein/extracellular signal-regulated kinase signal transducers of cell survival (Nebreda and Gavin, 1999) and cell-cycle regulation (Roux et al., 2003), whereas PAK kinases play key roles in the stimulation of mitogen-activated protein kinase signaling pathways (Kumar and Vadlamudi, 2002). RSKs phosphorylate an array of transcription factors (e.g., cAMP response element-binding protein, cAMP response element-binding protein/p300, estrogen receptor α, IκBα/nuclear factor-κBα, c-Fos),

TABLE 6
Summary of clone information

Clone	23	113
Gene Name	*RSK4*, also named *RPS6KA 6*	*PAK5*, also named *PAK7*
Localization	Chromosome X 1. intron	Chromosome 20 3. intron[a], site a, ChIP-confirmed, EMSA binding Site b, ChIP-confirmed, EMSA binding
Swiss-Prot/mRNA NCBI	Q9UK32/NM_014496	Q9P286/NM_045653
Reference	Yntema et al., 1999; Kohn et al., 2003	Pandey et al., 2002; Dan et al., 2002
mRNA Expression	Caco-2 cells, human liver, human brain, rat liver, rat brain, rat kidney	human liver, human brain, rat liver, rat brain, rat kidney
HNF4α Promoter Binding Sites	−1430 (prosite a), ChIP-confirmed, EMSA binding −2053 (prosite b), ChIP-confirmed, EMSA binding	−951 (prosite a), ChIP-confirmed, EMSA no binding −1766 (prosite b), EMSA binding −2181 (prosite c), ChIP-confirmed, EMSA no binding
Molecular Function	Protein kinase activity	Protein kinase activity
Biological Process	Cell communication/signal transduction	Cell communication/signal transduction

[a] Coincides with the 1. intron behind the 1. translated exon.

TABLE 7
HNF4α target regulation in STZ-induced diabetic rats and after Aroclor treatment
HNF4α, RSK4, and PAK5 gene expression was measured with real-time RT-PCR. Gene expression levels were normalized to mitATPase6.

Gene	Organ	Treatment	No. of Animals	Mean	S.D.	*p*
HNF4α	Liver	Control	8	0.85	0.29	
		STZ, 2 months	9	0.54	0.24	0.0288*
HNF4α	Kidney	Control	8	0.84	0.33	
		STZ, 2 months	7	0.55	0.10	0.0389*
RSK4	Kidney	Control	3	0.48	0.21	
		STZ, 6 months	3	0.36	0.08	0.0355**
RSK4	Kidney	Control	6	0.15	0.06	
		Aroclor 1257, 48 h	6	0.32	0.07	0.0015*
PAK5	Kidney	Control	8	0.12	0.06	
		STZ, 2 months	7	0.02	0.02	0.0015*
PAK5	Brain	Control	6	0.27	0.13	
		STZ, 2 months	7	0.13	0.07	0.0309*

* An unpaired two-tailed Student's *t* test was used to compare the treatment group against the control group.
** Analysis of covariance with interaction between factor and covariable was applied as a one-tailed test to compare the treatment group with the control group. The results were considered significant when the *p* value was less than 0.05.

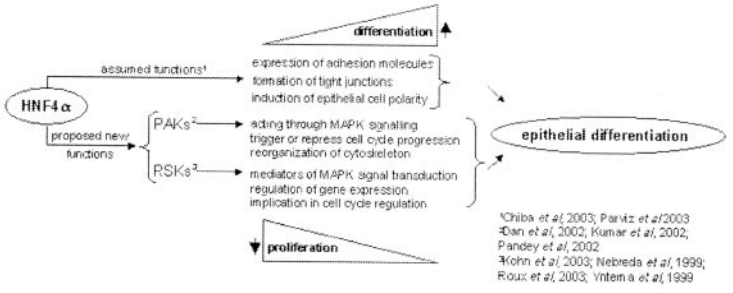

Fig. 3. Assumed function of HNF4α in cellular differentiation and cell-cycle control. For details, see text.

Downloaded from molpharm.aspetjournals.org by guest on December 1, 2012

take part in chromatin remodeling through phosphorylation of histone H3, and down-regulate $p34^{cdc2}$ inhibitory kinase, which may be important for progression through G_2/M phase of mitosis (Nebreda and Gavin, 1999). PAK kinases regulate cytoskeletal dynamics by disassembly of stress fibers and focal adhesions (Kumar and Vadlamudi, 2002). Its role in specific cellular cytoskeletal reorganization leads to the inhibition of cell spreading (Sanders et al., 1999). Thus, HNF4α targets two kinases that are indirect regulators of cell cycle, presumably with the aim of fostering cellular differentiation. In conclusion, we report a unique role for HNF4α in targeting RSK and PAK family members. This suggests a novel role for this liver-enriched transcription factor in repressing cell-cycle progression to enable cellular differentiation (Fig. 3). Recently, Chiba et al. (2005) reported that overexpression of HNF4α inhibited cell growth in F9 cells, and this was attributed to enhanced expression of cyclin-dependent kinase inhibitor $p21^{CIP1/WAF1}$, which supports the concept that HNF4α plays fundamental roles in the control of epithelial proliferation as well. Our data point to novel functions of HNF4α that are beyond the regulation of genes involved in hepatic metabolism. Further studies are now on the way to delineate the role of HNF4α in cell-cycle regulation and neuronal function. This may provide a missing link between HNF4α dysfunction and late-stage complications in diabetes frequently seen in patients with progressive stages of disease.

Acknowledgments

We thank S. Froese and A. Pfanne for valuable technical assistance, R. Zemlin for assistance in bioinformatics and advice on design of PCR primers, and K. Amann and P. Rösen for providing tissue of STZ-treated diabetic rats.

References

Bianchi R, Buyukakilli B, Brines M, Savino C, Cavaletti G, Oggioni N, Lauria G, Borgna M, Lombardi R, Cimen B, et al. (2004) Erythropoietin both protects from and reverses experimental diabetic neuropathy. *Proc Natl Acad Sci USA* **101:**823–828.

Borlak J and Thum T (2001) Induction of nuclear transcription factors, cytochrome P450 monooxygenases and glutathione S-transferase alpha gene expression in aroclor 1254-treated rat hepatocyte cultures. *Biochem Pharmacol* **61:**145–153.

Chen WS, Manova K, Weinstein DC, Duncan SA, Plump AS, Prezioso VR, Bachvarova RF, and Darnell JE Jr (1994) Disruption of the HNF-4 gene, expressed in visceral endoderm, leads to cell death in embryonic ectoderm and impaired gastrulation of mouse embryos. *Genes Dev* **8:**2466–2477.

Chiba H, Gotoh T, Kojima T, Satohisa S, Kikuchi K, Osanai M, and Sawada N (2003) Hepatocyte nuclear factor (HNF)-4alpha triggers formation of functional tight junctions and establishment of polarized epithelial morphology in F9 embryonal carcinoma cells. *Exp Cell Res* **286:**288–297.

Chiba H, Itoh T, Satohisa S, Sakai N, Noguchi H, Osanai M, Kojima T, and Sawada N (2005) Activation of $P21^{CIP1/WAF1}$ gene expression and inhibition of cell proliferation by overexpression of hepatocyte nuclear factor-4alpha. *Exp Cell Res* **302:**11–21.

Dan C, Nath N, Liberto M, and Minden A (2002) PAK5, a new brain-specific kinase, promotes neurite outgrowth in N1E-115 cells. *Mol Cell Biol* **22:**567–577.

Dhein S, Kabat A, Olbrich A, Rosen P, Schroder H, and Mohr FW (2003) Effect of chronic treatment with vitamin E on endothelial dysfunction in a type I in vivo diabetes mellitus model and in vitro. *J Pharmacol Exp Ther* **305:**114–122.

Dignam JD, Lebovitz RM, and Roeder RG (1983) Accurate transcription initiation by RNA polymerase II in a soluble extract from isolated mammalian nuclei. *Nucleic Acids Res* **11:**1475–1489.

Gorski K, Carneiro M, and Schibler U (1986) Tissue-specific in vitro transcription from the mouse albumin promoter. *Cell* **47:**767–776.

Greenbaum S and Zhuang Y (2002) Identification of E2A target genes in B lymphocyte development by using a gene tagging-based chromatin immunoprecipitation system. *Proc Natl Acad Sci USA* **99:**15030–15035.

Gross ML, El Shakmak A, Szabo A, Koch A, Kuhlmann A, Munter K, Ritz E, and Amann K (2003) ACE inhibitors but not endothelin receptor blockers prevent podocyte loss in early diabetic nephropathy. *Diabetologia* **46:**856–868.

Hayhurst GP, Lee YH, Lambert G, Ward JM, and Gonzalez FJ (2001) Hepatocyte nuclear factor 4alpha (nuclear receptor 2A1) is essential for maintenance of hepatic gene expression and lipid homeostasis. *Mol Cell Biol* **21:**1393–1403.

Horak CE, Mahajan MC, Luscombe NM, Gerstein M, Weissman SM, and Snyder M (2002) GATA-1 binding sites mapped in the β-globin locus by using mammalian chIp-chip analysis. *Proc Natl Acad Sci USA* **99:**2924–2929.

Hu C and Perlmutter DH (1999) Regulation of alpha1-antitrypsin gene expression in human intestinal epithelial cell line Caco-2 by HNF-1alpha and HNF-4. *Am J Physiol* **276:**G1181–G1194.

Jover R, Bort R, Gomez-Lechon MJ, and Castell JV (2001) Cytochrome P450 regulation by hepatocyte nuclear factor 4 in human hepatocytes: a study using adenovirus-mediated antisense targeting. *Hepatology* **33:**668–675.

Kohn M, Hameister H, Vogel M, and Kehrer-Sawatzki H (2003) Expression pattern of the Rsk2, Rsk4 and Pdk1 genes during murine embryogenesis. *Gene Expr Patterns* **3:**173–177.

Kumar R and Vadlamudi RK (2002) Emerging functions of P21-activated kinases in human cancer cells. *J Cell Physiol* **193:**133–144.

Li J, Ning G, and Duncan SA (2000) Mammalian hepatocyte differentiation requires the transcription factor HNF-4alpha. *Genes Dev* **14:**464–474.

Love-Gregory LD, Wasson J, Ma J, Jin CH, Glaser B, Suarez BK, and Permutt MA (2004) A common polymorphism in the upstream promoter region of the hepatocyte nuclear factor-4alpha gene on chromosome 20q is associated with type 2 diabetes and appears to contribute to the evidence for linkage in an Ashkenazi Jewish population. *Diabetes* **53:**1134–1140.

Martone R, Euskirchen G, Bertone P, Hartman S, Royce TE, Luscombe NM, Rinn JL, Nelson FK, Miller P, Gerstein M, et al. (2003) Distribution of NF-κB-binding sites across human chromosome 22. *Proc Natl Acad Sci USA* **100:**12247–12252.

Nakhei H, Lingott A, Lemm I, and Ryffel GU (1998) An alternative splice variant of the tissue specific transcription factor HNF4alpha predominates in undifferentiated murine cell types. *Nucleic Acids Res* **26:**497–504.

Nebreda AR and Gavin AC (1999) Perspectives: signal transduction. Cell survival demands some Rsk. *Science (Wash DC)* **286:**1309–1310.

Niehof M, Streetz K, Rakemann T, Bischoff SC, Manns MP, Horn F, and Trautwein C (2001) Interleukin-6-induced tethering of STAT3 to the LAP/C/EBPbeta promoter suggests a new mechanism of transcriptional regulation by STAT3. *J Biol Chem* **276:**9016–9027.

Pandey A, Dan I, Kristiansen TZ, Watanabe NM, Voldby J, Kajikawa E, Khosravi-Far R, Blagoev B, and Mann M (2002) Cloning and characterization of PAK5, a novel member of mammalian P21-activated kinase-II subfamily that is predominantly expressed in brain. *Oncogene* **21:**3939–3948.

Parviz F, Matullo C, Garrison WD, Savatski L, Adamson JW, Ning G, Kaestner KH, Rossi JM, Zaret KS, and Duncan SA (2003) Hepatocyte nuclear factor 4alpha controls the development of a hepatic epithelium and liver morphogenesis. *Nat Genet* **34:**292–296.

Roux PP, Richards SA, and Blenis J (2003) Phosphorylation of P90 ribosomal S6 kinase (RSK) regulates extracellular signal-regulated kinase docking and RSK activity. *Mol Cell Biol* **23:**4796–4804.

Sanders LC, Matsumura F, Bokoch GM, and de Lanerolle P (1999) Inhibition of myosin light chain kinase by P21-activated kinase. *Science (Wash DC)* **283:**2083–2085.

Schrem H, Klempnauer J, and Borlak J (2002) Liver-enriched transcription factors in liver function and development. Part I: the hepatocyte nuclear factor network and liver-specific gene expression. *Pharmacol Rev* **54:**129–158.

Sladek FM and Seidel SD (2001) Hepatocyte nuclear factor 4alpha, in *Nuclear Receptors and Disease* (Burris T and McCabe ERB eds) pp 309–361, Academic Press, London.

Solano PJ, Mugat B, Martin D, Girard F, Huibant JM, Ferraz C, Jacq B, Demaille J, and Maschat F (2003) Genome-wide identification of in vivo *Drosophila* engrailed-binding DNA fragments and related target genes. *Development* **130:**1243–1254.

Soutoglou E and Talianidis I (2002) Coordination of PIC assembly and chromatin remodeling during differentiation-induced gene activation. *Science (Wash DC)* **295:**1901–1904.

Tomaru Y, Kondo S, Suzuki M, and Hayashizaki Y (2003) A comprehensive search for HNF-3[Alpha]-regulated genes in mouse hepatoma cells by 60K cDNA microarray and chromatin immunoprecipitation/PCR analysis. *Biochem Biophys Res Commun* **310:**667–674.

Vinik AI, Park TS, Stansberry KB, and Pittenger GL (2000) Diabetic neuropathies. *Diabetologia* **43:**957–973.

Weinmann AS, Bartley SM, Zhang T, Zhang MQ, and Farnham PJ (2001) Use of chromatin immunoprecipitation to clone novel E2F target promoters. *Mol Cell Biol* **21:**6820–6832.

Yntema HG, van den Helm B, Kissing J, van Duijnhoven G, Poppelaars F, Chelly J, Moraine C, Fryns JP, Hamel BCJ, and Heilbronner H (1999) A novel ribosomal S6-kinase (RSK4; RPS6KA6) is commonly deleted in patients with complex X-linked mental retardation. *Genomics* **62:**332–343.

Address correspondence to: Dr. Jürgen Borlak, Fraunhofer Institute of Toxicology and Experimental Medicine, Center for Drug Research and Medical Biotechnology, Nikolai-Fuchs-Str. 1, 30625 Hannover, Germany. E-mail: borlak@item.fraunhofer.de

MOL PHARM
MOLECULAR PHARMACOLOGY
aspet
Downloaded from molpharm.aspetjournals.org by guest on December 1, 2012